

# RSC Advances



This is an *Accepted Manuscript*, which has been through the Royal Society of Chemistry peer review process and has been accepted for publication.

*Accepted Manuscripts* are published online shortly after acceptance, before technical editing, formatting and proof reading. Using this free service, authors can make their results available to the community, in citable form, before we publish the edited article. This *Accepted Manuscript* will be replaced by the edited, formatted and paginated article as soon as this is available.

You can find more information about *Accepted Manuscripts* in the [Information for Authors](#).

Please note that technical editing may introduce minor changes to the text and/or graphics, which may alter content. The journal's standard [Terms & Conditions](#) and the [Ethical guidelines](#) still apply. In no event shall the Royal Society of Chemistry be held responsible for any errors or omissions in this *Accepted Manuscript* or any consequences arising from the use of any information it contains.

1    **Electrochemical treatment of mature landfill leachate using**  
2    **Ti/RuO<sub>2</sub>-IrO<sub>2</sub> and Al electrode: optimization and mechanism**

3    Juan Li <sup>a,b</sup>, Zhao-hui Yang <sup>a,b,\*</sup>, Hai-yin Xu <sup>a,b</sup>, Pei-pei Song <sup>a,b</sup>, Jing Huang <sup>a,b</sup>, Rui Xu  
4    <sup>a,b</sup>, Yi-jie Zhang <sup>a,b</sup>, Yan Zhou <sup>a,b</sup>

5    <sup>a</sup> College of Environmental Science and Engineering, Hunan University, Changsha  
6    410082, PR China

7    <sup>b</sup> Key Laboratory of Environmental Biology and Pollution Control (Hunan  
8    University), Ministry of Education, Changsha 410082, PR China

9    \* Corresponding author at: College of Environmental Science and Engineering, Hunan  
10   University, Changsha 410082, PR China. Tel: +86 0731 88822829;  
11   fax: +86 0731 88822829  
12   E-mail address: yzh@hnu.edu.cn (Z.-h. Yang).

## Abstract

Today, improving the elimination of refractory pollutants in landfill leachate through electrochemical oxidation technology has attracted considerable attention. In this study, a combination of anodic oxidation and cathodic coagulation process using Ti/RuO<sub>2</sub>-IrO<sub>2</sub> and Al electrode, was adopted to treat the mature landfill leachate with a very low biodegradability ratio (BOD<sub>5</sub>/COD) of 0.12. The effects of current density, pH, and the chloride ion concentration on the removal of chemical oxygen demand (COD) and ammonia nitrogen (NH<sub>3</sub>-N) were investigated by response surface methodology (RSM). The optimum condition of 83.7% COD and 100% NH<sub>3</sub>-N removal was achieved at current density 0.1 A/cm<sup>2</sup>, pH 6.37, the chloride ion concentration 6.5 g/L, and electrolytic time 150 min. In addition, heavy metals were partly removed. A main degradation mechanism of pollutants, including oxidation, coagulation and precipitation, was elucidated by Gas chromatography-mass spectrometry (GC-MS), Environmental scanning electron microscopy coupled with Energy dispersive spectrometer (ESEM/EDS) and Fourier transform infrared spectroscopy (FT-IR) analysis of organic components in landfill leachate and sludge generated in cathode. These results indicated that the electrochemical processes could be a convenient and efficient method for the treatment of landfill leachate.

**Keywords:** Leachate; Chemical oxygen demand; Ammonia nitrogen; Oxidation; Coagulation;

## 33 1. Introduction

34 Rapid economic development and population growth followed by inadequate  
35 infrastructure, expertise, and land scarcity have resulted in an increase in the amount  
36 of municipal solid waste (MSW)<sup>1,2</sup>. Even if there are many options for municipal  
37 solid waste management, sanitary landfill remains the most common and desirable  
38 management strategy due to low cost, simple procedures and landscape restoring  
39 effect on holes from mineral working<sup>3</sup>. But the secondary pollution of concomitant  
40 landfill leachate has become one of the most critical environmental issues<sup>4</sup>. Generally,  
41 landfill leachate can be considered complex and a high-polluting strength wastewater  
42 that possesses suspended solids, nitrogen compounds, various types of organic  
43 compounds and heavy metals<sup>5</sup>. The composition and concentration are mainly  
44 dependent on the type of waste and the age of the landfill<sup>6</sup>. Among them, the high  
45 concentration of chemical oxygen demand (COD) and ammonia nitrogen (NH<sub>3</sub>-N) are  
46 the key factors<sup>7</sup>. If without any appropriate treatment, landfill leachate contributes to  
47 severe pollutions to the receiving water bodies, likewise imparts adverse impact on  
48 ecosystem and public health<sup>8</sup>. Thus, environmental regulations require that the  
49 leachate must be pretreated on site to meet the standards for its discharge into the  
50 sewer or surface water.

51 Because of recalcitrant NH<sub>3</sub>-N and relatively low five-day biological oxygen  
52 demand (BOD<sub>5</sub>)/chemical oxygen demand (COD) ratio, mature landfill leachate (>10  
53 years)<sup>9</sup> can not be treated by conventional biological treatment, such as aerobic and

anaerobic biological degradation<sup>10</sup>. However, the electrochemical oxidation process with high effectiveness, environmental compatibility and easy in operation has been shown as a promising alternative for NH<sub>3</sub>-N removal<sup>11</sup>. In the electrochemical oxidation<sup>12</sup>, employing different types of anode materials plays a dominant role, and substantially influences both reaction selectivity and efficiency<sup>13, 14</sup>, such as Ti, PbO<sub>2</sub>/Ti, RuO<sub>2</sub>, Fe, Al, and boron-doped diamond (BDD), etc<sup>15</sup>. Among the various anodes used, RuO<sub>2</sub> and IrO<sub>2</sub> coated Ti anode (Ti/RuO<sub>2</sub>-IrO<sub>2</sub>) stands out, which has been utilized widely with well-proven advantages<sup>16</sup>. It possesses high stability and catalytic activity, not only for chlorine evolution, but also for oxygen evolution. Several authors have applied Ti/RuO<sub>2</sub>-IrO<sub>2</sub> electrode to the treatment of landfill leachate<sup>3</sup>. Usually, cathode is protected against corrosion in the electrooxidation technology. Except for a carrier of the electronic, it does not have substantial effect. On the contrary, taking advantage of the cathode corrosion and investigating the effect in the solution have a certain significance. As the third most abundant element in the earth crust, aluminum and its alloys are recognized to be one of the most suitable metals for future hydrogen production, energy storage and conversion<sup>17, 18</sup>. Moreover, aluminium as the cathode can produce hydroxide at the expense of sacrificial aluminum, which has a promoting coagulation effect on pollutant removal<sup>17</sup>. In consequence, we can construct electrooxidation and coagulation into a system to further improve the efficiency of processing, which has not been studied yet. When anodic oxidation is combined with the cathodic coagulation, structure of reaction tank

75 can be optimized. Compared with the pure electrochemical oxidation, the removal  
76 rate of pollutants is improved significantly.

77 In this study, mature landfill leachate was treated by the combination of  
78 electrooxidation-coagulation processes using Ti/RuO<sub>2</sub>-IrO<sub>2</sub> anode and Al cathode. The  
79 main objectives can be divided into three aspects. Firstly, the effects of various  
80 operating variables e.g. electrolytic time, electrode gap, current intensity, pH and  
81 initial concentration of chloride ions on COD, NH<sub>3</sub>-N, colour and heavy metals  
82 removal were investigated. In parallel, response surface methodology (RSM) was  
83 considered to be an effective means to evaluate their interactions and determine the  
84 optimum operational conditions <sup>10</sup>. Secondly, some associated mechanisms were  
85 presented, regarding oxidation and coagulation that occurred in the electrode/solution  
86 boundary. Finally, energy consumption was used to examine its performance in the  
87 electrochemical process.

## 88 **2. Materials and methods**

### 89 **2.1 Materials**

90 The used leachate was sampled from Heimifeng Landfill located in Changsha  
91 (China). It has been running since 2003. This plant covers about 174 ha surface and  
92 treats more than 3000 tons solid waste daily. Table 1 provided a general  
93 physicochemical characteristics of the raw leachate in accordance with the standard  
94 methods <sup>19</sup>. As could be seen, the raw leachate presented with a black color, which  
95 was associated with a high organic pollutant charge, high ammonia nitrogen content,

96 and a low BOD<sub>5</sub>/COD (0.12) ratio. It could be categorized as mature landfill leachate  
97 because of low biodegradability. There was a high concentration of chlorine, sodium  
98 and potassium within this leachate, which led to a high conductivity of 12.62 mS cm<sup>-1</sup>,  
99 permitting the application of electrochemical process. It also contained a relatively  
100 low concentration of toxic heavy metals, which tended to accumulate in the biological  
101 organisms.

## 102 2.2 Experimental procedures

103 The experimental setup was shown in Fig. 1. In this study, electrodes with surface  
104 area of 35cm<sup>2</sup> (= Anode: Ti/RuO<sub>2</sub>-IrO<sub>2</sub>; Cathode: Al), were placed vertically and  
105 parallel to each other in the electrolytic reactor containing 500 mL of leachate sample.  
106 A precision digital direct current power supply (DC, 0~32V, 0~5A) was used to  
107 provide the desired current. Initial pH was adjusted with concentrated nitric acid or  
108 sodium hydroxide. Solid sodium chloride (NaCl), as electrolyte was added before  
109 each experiment. The reactor was placed on a magnetic stirring block at a maintained  
110 speed of 200 rpm, in order to keep its contents well mixed during the experiment.  
111 Besides, all experiments were conducted at room temperature and atmospheric  
112 pressure. After each run, the sample was settle down for 20 min and the supernatant  
113 was taken to make analysis.

## 114 2.3 RSM experimental design

115 Response surface methodology (RSM) was an experimental technique used for  
116 predicting and modeling complicated relationship between independent factors and

one or more responses<sup>20</sup>. Additionally, it could reduce the number of runs in comparison with the orthogonal experiment method. Central composite design (CCD), a branch of RSM, was appropriate to fit a quadratic model, as well as to select optimal condition of variables and predict the best value of responses<sup>21</sup>. Operating between the responses of the corresponding coded values and the different process variables, the response model might be expressed by a second-degree polynomial equation as illustrated in Eq. (1):

$$y = b_o + \sum_{i=1}^m b_i x_i + \sum_{i < j}^m b_{ij} x_i x_j + \sum_{i=1}^m b_{ii} x_i^2 \quad (1)$$

Where  $y$  is the response variable,  $b_o$  is a constant,  $b_i$ ,  $b_{ii}$ , and  $b_{ij}$  are the linear, quadratic, and interaction coefficients, respectively.  $x_i$  and  $x_j$  are independent variables ( $i \neq j$ ).

On the basis of the single factor test results, three independent variables (current density ( $x_1$ ), pH ( $x_2$ ) and the chloride ion concentration ( $x_3$ )) and two responses (COD and NH<sub>3</sub>-N removal) were investigated in this experiment. The practical design parameters and their levels were presented in Table 2, with the help of the Design Expert software (Version 8.0.6, Stat-Ease Inc, Minneapolis, MN). Then, it was also used for handle of the experimental data to obtain the equations and analysis of variance (ANOVA)<sup>10</sup>. The test of statistical significance must be based on the total error criteria with a confidence level of 95.0% ( $p < 0.05$ ).  $R^2$ , which ranged from 0 to 1, was used to express the fit quality of the polynomial model equation. When  $R^2$  value closer to 1, it meant the model was more accurate. Three dimensional (3D)



response surface plots were constructed from the developed models in order to study the individual and interactive effect of the process variables on the responses. And all response surface plots have clear peaks, meaning that the optimum conditions were located to find out maximum values of the responses.

#### 2.4 Analysis and calculations

The instruments used to measure conductivity and pH were conductivity meter (DDS-11A, Shanghai) and pH meter (HI 98184, HANNA, Italy), respectively. Levels of chloridion was measured using silver nitrate titration method according to the standard methods<sup>19</sup>. Used for the performance evaluation, COD was determined by a fast digestion-titration method based on the potassium dichromate, and NH<sub>3</sub>-N was determined spectrophotometrically using the Nesslerisation method at an absorbance of 425 nm. The concentration of heavy metals in the solution were analyzed by inductively coupled plasma-atomic emission spectrometry (ICP-AES, PS-6, Barid Company, US). Organic composition was determined by gas chromatography-mass spectrometry equipment (GC/MS, Model QP-2010, Shimadzu, Japan). Environmental scanning electron microscopy (ESEM) coupled with Energy dispersive spectrometer (EDS) (Quanta 200 FEG, FEI, US) and Fourier transform infrared spectroscopy (FTIR-8400S, IRprestige-21) were chosen to characterize the sludge generated in experiment.

The percentage removal of pollutant in the aqueous solution was calculated by using Eq. (2):

$$\text{Removal rate} = \frac{C_o - C_e}{C_o} \times 100\% \quad (2)$$

where  $C_o$  and  $C_e$  are the initial and final concentration, respectively.

Electric energy per mass,  $E_{EM}$  (kWh/kg<sup>-1</sup>), was proposed by Bolton to judge economic feasibility, whether was suitable for large scale application<sup>22</sup>. It was defined as the electric energy in kilowatt-hour (kWh) required to degrade a kilogram of a specific pollutant in contaminated water, as described by Eq. (3):

$$E_{EM} = \frac{UIt}{(C_o - C_e)V} \quad (3)$$

where  $E_{EM}$  is the electrical energy consumption (KWh/kg),  $U$  is the potential (V),  $I$  is the current (A),  $t$  is the time (h),  $V$  is the volume of the solution treated (L),  $C_o$  (mg/L) and  $C_e$  (mg/L) are the concentrations of pollutants before and after electrochemical process.

### 3. Results and discussion

#### 3.1 Factors influencing COD and NH<sub>3</sub>-N removal

As exemplified by Fig. 2(a), Al cathode showed higher rates for COD and NH<sub>3</sub>-N removal than that of Ti/RuO<sub>2</sub>-IrO<sub>2</sub>. This could be explained by the fact that chemical dissolution of aluminum occurred when the aluminum was polarized cathodically. Al cathode transferred higher numbers of Al<sup>3+</sup> into the solution and they produced a higher amount of sludge. And these sludge had a coagulation effect on pollutants in the landfill leachate. The phenomenon also referred to as “chemical dissolution” or “cathodic corrosion”<sup>17</sup>, which was contribute to color removal meanwhile and 100%

179 efficiency were observed in Fig. 2(b). From the above, our subsequent experiment  
180 focused on Ti/RuO<sub>2</sub>-IrO<sub>2</sub> anode and Al cathode.

181 On the other hand, Fig. 2(a) showed the influence of reaction time on the COD and  
182 NH<sub>3</sub>-N removal rate when it was varied from 0 to 180 min. Electrolytic time had a  
183 positive effect on mineralization and decolorization of leachate. It was noted that the  
184 maximum COD and NH<sub>3</sub>-N removal was obtained with an optimal electrolytic time of  
185 about 150 min. When the allowed reaction time longer than 150 min, the removal rate  
186 were not further improved considerably.

187 In a parallel-plate monopolar reactor, the electrical field and conductivity could be  
188 controlled by varying electrode gap<sup>23</sup>. In order to investigate the effect of  
189 inter-electrode distance on the efficiency of the process, the reactor was arranged such  
190 that electrodes were positioned at 1 cm to 6 cm. Fig. 2(c) showed the COD and  
191 NH<sub>3</sub>-N removal rates obtained from different distances. We could conclude that COD  
192 and NH<sub>3</sub>-N removal rates increased with an increase in electrode gap, until it was 5  
193 cm. This might be related to diffusion limitations at small gap system. Subsequently,  
194 the removal rates was decreased. This suggested that the resistivity of the solution  
195 increased and it will reduce the mass transfer efficiency. Hence, the recommended gap  
196 in our experiment was 5 cm, which was kept constant in all experiments.

### 197 3.2 RSM design

#### 198 3.2.1 Quadratic model

199 According to the RSM results in regard to the response variables of COD and

NH<sub>3</sub>-N removal, which were acquired from 20 groups of experiments with the help of Design-Expert software, the final optimum fit model equations were obtained as follows:

COD removal rate:

$$y_1 = 52.91 + 9.40x_1 - 9.46x_2 - 2.81x_3 + 0.33x_1x_2 + 1.46x_1x_3 + 1.23x_2x_3 + 3.68x_1^2 + 0.84x_2^2 + 0.33x_3^2$$

(4)

NH<sub>3</sub>-N removal rate:

$$y_2 = 76.74 + 18.33x_1 + 11.54x_2 + 1.44x_3 + 3.62x_1x_2 + 3.67x_1x_3 - 2.70x_2x_3 - 3.95x_1^2 - 5.03x_2^2 - 0.29x_3^2$$

(5)

On the basis of the experimental values, statistical testing was carried out using Fisher's test for ANOVA of regression parameters in quadratic model. Results were listed in Table 3 and indicated the second-order equation fitted well. Because the Prob > F of model was less than 0.05, and total determination coefficient R<sup>2</sup> of COD and NH<sub>3</sub>-N reached 0.9535, 0.9749, respectively.

### 3.2.2 Interaction between variables

Fig. 3(a) and Fig. 3(d) clearly represented the effects of current density ( $x_1$ ) and pH ( $x_2$ ) on the COD and NH<sub>3</sub>-N removal, while the chloride ion concentration ( $x_3$ ) was fixed. It indicated that the COD and NH<sub>3</sub>-N removal rates increased significantly when the current density was increased upto 0.1 A/cm<sup>2</sup>. Thereafter, there was a negligible effect on removal rates of COD and NH<sub>3</sub>-N. This was attributed to the

220 higher formation of hydroxyl radicals species ( $\text{OH}\cdot$ ) that was controlled by the  
221 applied current during electrolysis.  $\text{OH}\cdot$  had the strong positive effects on the organic  
222 matters presented in the landfill leachate, thus the removal rates were increased<sup>16</sup>. pH  
223 was a very important parameter for electrochemical degradation of COD and  $\text{NH}_3\text{-N}$   
224 in landfill leachate. Under the acidic condition, the removal rate of COD was  
225 relatively high. In neutral or alkaline solution, it was more suitable for removal of  
226  $\text{NH}_3\text{-N}$ . The reasons could be as follows. Firstly, the amounts of  $\text{OH}\cdot$  were large at  
227 low pH, which could accelerate the mineralization of COD. Besides, small molecule  
228 organic matters were easier to be eliminated than  $\text{NH}_3\text{-N}$  with larger radius. Secondly,  
229 in high pH, organic matters were in stable non-dissociation state and hard to be  
230 removed. Nevertheless, the proportion of ammonia in the form of  $\text{NH}_3 \cdot \text{H}_2\text{O}$  which  
231 could be stripped out of solution was improved<sup>24</sup>.

232 Fig. 3(b) showed COD and  $\text{NH}_3\text{-N}$  removal with the variation of current density  
233 ( $x_1$ ) and the chloride ion concentration ( $x_3$ ), as well as the interaction between them.  
234 With current density at low levels, COD removal was higher with the decrease of the  
235 chloride ion concentration owing to the decrease of oxidation capacity of anode in  
236 high NaCl dosage. On the contrary, with current density at high levels, the higher  
237 removal of COD was obtained at high chlorine ion concentration. That was probably  
238 because more active free chlorine could be generated by increasing the current density  
239 and chloride concentration simultaneously, according to Czarnetzki and Janssen  
240 reported<sup>25</sup>. It was obviously seen that the  $\text{NH}_3\text{-N}$  removal exhibit the same tendency,

241 as shown in the Fig. 3(e).

242 Fig. 3(c) presented the interaction between pH ( $x_2$ ) and the chloride ion  
243 concentration ( $x_3$ ) and their effects on the COD and NH<sub>3</sub>-N removal. Increasing the  
244 chloride ion concentration ( $x_3$ ) to 4.5 g/L at a range from 5 to 7 for the pH ( $x_2$ )  
245 decreased COD removal rate, whereas further increase in the chloride ion  
246 concentration ( $x_3$ ) made the removal rate of COD remain unchanged. From 7 to 9 of  
247 the pH ( $x_2$ ), the chloride ion concentration increasing was usually accompanied a  
248 moderate but significant acceleration of treatment rate in terms of COD removal.  
249 Previous studies showed similar results of various electrolytes like NaCl, KCl, NaNO<sub>3</sub>,  
250 NaSO<sub>4</sub>, etc <sup>26</sup>. But, due to low cost and easy availability, NaCl was worthy of being  
251 selected as the best electrolyte <sup>27</sup>. For NH<sub>3</sub>-N removal shown in Fig. 3(f), there was  
252 the just the opposite with the COD removal results.

253 As can be seen in Fig. 3, average removal rate of NH<sub>3</sub>-N were higher than COD  
254 during the electrolysis, which was agreement with the reports by Chiang <sup>28</sup> and Feki et  
255 al <sup>29</sup>. During the electrochemical process, both COD and NH<sub>3</sub>-N could be removed  
256 simultaneously and there would be a competition between them yet. According to the  
257 report by Deng and Englehardt, the rule of competition between removal of COD and  
258 NH<sub>3</sub>-N seemed to be that the removal of NH<sub>3</sub>-N was greater than that of COD when  
259 indirect oxidation was prevalent, whereas COD removal took priority under direct  
260 anodic oxidation <sup>30</sup>.

261 3.2.3 Optimization of the electrolysis process

262 According to RSM, the optimized conditions occurred at current density  $0.1 \text{ A/cm}^2$ ,  
263 pH 6.37, the chloride ion concentration  $6.5 \text{ g/L}$ , reaction time 150 min and electrode  
264 gap 5 cm. which should result in COD removal of 84.26% and  $\text{NH}_3\text{-N}$  removal of  
265 100%. In order to confirm the accuracy and reliability of the predicted value, an  
266 experiment was then conducted. Table 4 showed that the experimental values were  
267 fitted well with the predicted ones, and COD and  $\text{NH}_3\text{-N}$  removal rates were 83.93%  
268 and 100% respectively. It also confirmed that RSM was a powerful tool for  
269 optimizing the operational conditions of electrochemical experiment with great  
270 accuracy. Comparing the performance of the other cathode material systems in the  
271 literatures<sup>31-37</sup>, which showed in table 5, we could reasonably conclude that Al was  
272 more superior to COD and  $\text{NH}_3\text{-N}$  removal carried out at less time.

273 Besides enhanced the treatment efficiency of COD and  $\text{NH}_3\text{-N}$ , this procedure also  
274 had the potential to eliminate possible heavy metals, like chromium, zinc and part of  
275 the aluminum introduced during the cathodic corrosion process. A number of studies  
276 demonstrated the natural attenuation of heavy metals within a landfill. However, there  
277 were many varieties of heavy metals in landfill leachate, such as Fe, B, Al, Ni, Zn, Cr,  
278 As, Pb, Co, Se, and Cu, the concentration of which was relatively low, as shown in  
279 Table 6. After 150 min electrolytic time on the optimal conditions, the removal rates  
280 of heavy metals comparing with the initial concentrations were 99.60%, 28.57%,  
281 100.00%, 93.33%, 16.67%, 33.33%, 95.00%, 90.00%, 100.00%, 80.00%, and  
282 100.00%, respectively. These results could be explained with respect to cathode

corrosion, where sludge provided functional groups ( hydroxyl) on the large surface to remove heavy metals through electrostatic absorption or frequent coagulation <sup>38</sup>.

### 3.3 Mechanism analysis

In the following subsections, a detailed description of these mechanisms that responsible for pollutants removal during the combination of electrooxidation and coagulation processes of landfill leachate, was going to be carried out by GC-MS, ESEM/EDS and FT-IR analysis of organic components in landfill leachate and sludge generated in cathode .

#### 3.3.1 Analysis of organic compounds in landfill leachate

In order to gain insight into the organics in the leachate before and after electrochemical experiment, leachate contents in the influent and effluent of the electrochemical reactor were analyzed by the gas chromatography-mass spectrometry system (GC-MS) <sup>39</sup>. There were 109 kinds of organic pollutants detected in the original landfill leachate, whose match percent was not less than 85%, including acids, esters, cyclic ketone, the long-chain hydrocarbons, etc. As shown in Fig. 4, it was evident that the species and mass percentage of organic compounds in landfill leachate were found to have considerably declined during electrochemical process. However, some new compounds were detected in the effluent of the electrochemical reactor. These results implied that it produced refractory matter which were difficult to remove absolutely, when strong oxidant convert macromolecular organic to small molecule organic <sup>40</sup>.



### 3.3.2 Characterization of sludge

Knowing the crystalline structures and composition of sludge that produced from aluminum cathode would provide valuable information, regarding the fundamental mechanisms of pollutants removal. To evaluate the structural features, ESEM image and EDS spectra of particles sludge were performed. As illustrated in Fig. 5(a), ESEM image displayed the presence on the surface of mostly amorphous or ultrafine particular structure at micrometer size. In Fig. 5(b), the detected elements analysis by EDS indicated that the surface of these particles was coated with a layer of contaminant, most likely C, O, and Al species. These results confirmed the existence of cathode corrosion process and it was helpful to remove pollutants presented in the solution.

Fig. 5(c) showed FT-IR spectra of sludge in the 500~4000  $\text{cm}^{-1}$  range, which revealed formation of new species in electrochemical process. From curve, apparition of a peak at 528.5  $\text{cm}^{-1}$ , 657.73  $\text{cm}^{-1}$  at 1377.17  $\text{cm}^{-1}$  were ascribed to Al-OH, Al-O and Al-H bending, which were characteristic of  $\text{Al}(\text{OH})_3$  or  $\text{Al}(\text{OH})_4^{-}$ . As a coagulant, hydroxides of aluminum could be considered the responsible constituent of heavy metals removal. Additionally, peaks 1419.61  $\text{cm}^{-1}$  and 1637.56  $\text{cm}^{-1}$  were also observed corresponding to -COOH stretching and H-O-H bending respectively. C-H vibration in aromatic structures was represented by the band at 3051.39  $\text{cm}^{-1}$ . These indicated the part of organic pollutants in landfill leachate might be adsorbed on coagulant surface. It also had absorbance bands with maxima at 3442.94  $\text{cm}^{-1}$

representing O–H stretching of hydroxyl groups from hydrogen bonding<sup>43</sup>. Thus, all of these showed that coagulation process due to the cathodic corrosion were successfully remove some pollutants.

### 3.3.3 Reaction mechanism

Fig. 6 showed the reaction mechanism responsible for the removal of pollutants. As the reaction progresses, the evolution of pH and the chloride ion concentration (Fig. 7) were found to be inter-related, which can be interpreted in terms of the electrochemical and the chemical reactions. As follows, the species within the solution participated in the reactions in a different manner.

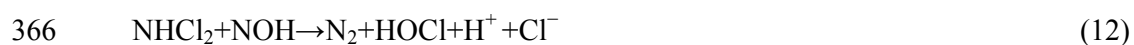
In anode: Pollutions removal in the presence of electrolyte (NaCl) were carried out in two ways viz:

(i) Direct oxidation: On Ti/RuO<sub>2</sub>-IrO<sub>2</sub> anode, almost complete mineralization of some organic matter with very high current density was obtained, which occurred through direct electron transfer in the potential region. In addition, hydroxyl radicals or other reactive species were generated from water electrolysis owing to the high overpotential for oxygen production, and participated in the electrochemical oxidation at the anode surface<sup>39</sup>. They could promote the oxidation/reduction reactions of the organic pollutants, contained in the electrochemical cell, which improved the removal of large recalcitrant organic molecules or transformed them into more easily biodegradable substances<sup>44</sup>. This property led to an excellent COD removal efficiency.

(ii) Indirect oxidation: With the chloride ion concentration, the ability of electric conduction could be improved and the passivation of the electrode could be relieved. Moreover, chloride ions also competed with organic matter to be oxidized at the anode<sup>45</sup>. During the electrochemical process, the chlorid ion ( $\text{Cl}^-$ ) would be discharged at the anode to generate dissolved gas chlorine ( $\text{Cl}_2$ ), then the  $\text{Cl}_2$  could be chemically converted to hypochlorite ion ( $\text{OCl}^-$ ). This was the reason for that the chloride ion concentration in the solution had been decreased, until reached a constant value. The possible reactions occurring were listed below:



The sum of the three species:  $\text{Cl}^-$ ,  $\text{Cl}_2$ , and  $\text{ClO}^-$  were termed free chlorine. In the normal pH range of pond water (6~7.5),  $\text{ClO}^-$  was the major component of free chlorine. In turn, as "active chlorine" possessing a high stability and oxidation capacity,  $\text{OCl}^-$  could accelerate the mineralization of organics effectively. In this case,  $\text{NH}_3\text{-N}$  in the leachate could be also removed preferentially through the mechanism similar to "breakpoint reactions"<sup>46</sup>:



367 On the whole, both direct and indirect oxidations were involved in COD and  
368  $\text{NH}_3\text{-N}$  removal. And COD removal by direct oxidation occurred at a higher rate than  
369 that of  $\text{NH}_3\text{-N}$ , while indirect oxidation preferred removal of  $\text{NH}_3\text{-N}$  than that of COD.

370 In cathode: Picard et al <sup>47</sup> showed that there was a chemical attack on the aluminum  
371 cathode by hydroxide ions generated during water reduction Eq.(13), leading to  
372 increase of the pH essentially. It was well established that the dissolution occurred  
373 through the intermediate of an oxide/hydroxide film <sup>18</sup>, which was formed  
374 spontaneously and existed on the surface of aluminium. As expressed by Eq.(14,15),  
375 aluminum cation along with  $\text{OH}^-$  ion formed a hydroxide of a network structure, large  
376 surface area and high absorption. As colloid coagulant, mainly at pH values in the  
377 range of 6.0-7.0, they promoted the generation of sweep flocs inside the treated  
378 wastewater, whose enmeshment made pollutants removed. Once the colloidal matter  
379 was destabilized, it could be separated from the wastewater. In addition to COD and  
380  $\text{NH}_3\text{-N}$  removal, this mechanism played a key role in removal of heavy metals from  
381 landfill leachate. It was found that the corrosion rate of aluminium increased during  
382 cathodic polarization, being coupled with the hydrogen evolution arising from the  
383 attack by hydroxide ions near the electrode surface. And the amount of hydroxide  
384 generated in the process was strongly influenced by the pH and the current density.  
385 Aluminum had a very low corrosion rate in neutral solutions due to the formation of  
386 an insoluble passive film, but the rapid cathodic aluminum dissolution could be  
387 observed in low or high pH electrolytes, which was in a good agreement with the

388 results of Moon and Pyun<sup>18, 48</sup>. It was also noted that the corrosion rate increases with  
389 increasing applied cathodic current density. These could justify the important  
390 contribution of the chemical dissolution of aluminum in the cathode to the COD,  
391 NH<sub>3</sub>-N and heavy metals removal.



### 395 3.4 Economic evaluation

396 The technical feasibility of the electrochemical process was usually evaluated in  
397 terms of the percentage removal of pollutants reached, while the economic feasibility  
398 was determined by the energy consumption. Typical costs in landfill leachate  
399 treatment with the combination of electrooxidation-coagulation processes were the  
400 expenditure on energy consumption, mass loss of electrodes and the chemical addition  
401 <sup>22</sup>. Among them, chemical addition was only used for the purpose of initial pH  
402 adjustment and additional electrolyte, whose dosage was reasonably few. Thus, it was  
403 out of the scope of the present work.

404 In Fig. 8, it reported the variation of specific energy consumption, as function of  
405 COD and NH<sub>3</sub>-N removal, in the optimum operating condition found previously. For  
406 low current density, the specific energy consumption increases almost linearly, while  
407  $E_{EM}$  (COD) increased slowly and  $E_{EM}$  (NH<sub>3</sub>-N) increased sharply for high current  
408 density. This behaviour could be probably explained by the decrease of organic

content or the formation of more refractory product in the solution. Under the optimum conditions, the electrochemical treatment for 1 kg COD and 1 kg NH<sub>3</sub>-N in landfill leachate required the power consumption of 61.59 kWh and 106.91 kWh respectively, which was close to other studies <sup>2</sup>. Additionally, the mass loss of an aluminum electrode for a liter of leachate being treated was 0.46 g.

#### 4. Conclusions

This study demonstrated that when the combination of Ti/RuO<sub>2</sub>-IrO<sub>2</sub> and Al electrode, they could achieve a significant synergy. The process was found to had an excellent removal performance for COD, NH<sub>3</sub>-N, colour and heavy metals in landfill leachate, and could effectively reduce the contaminant loading of these effluents and enhance biodegradability, improved from a BOD<sub>5</sub>/COD ratio of 0.12 to 0.38.

Observed the effects of variables using RSM, an optimal operating condition were found to be: current density of 0.1 A/cm<sup>2</sup>, pH of 6.37, the chloride ion concentration of 6.5g/L, electrolysis time 150 min and electrode gap 5 cm, respectively. Under these conditions, the removal rates of COD and NH<sub>3</sub>-N were found to be 83.93% and 100%, respectively, which were consistent with the overlay plot results. Therefore, RSM could be effectively adopted to optimize the operating multifactor in complex electrochemical process. In addition, the behaviors of COD, NH<sub>3</sub>-N and heavy metals removal were investigated. The predominant mechanisms included oxidation, coagulation and precipitation, confirmed by GC-MS, ESEM/EDS and FTIR analyses.

In most cases, a single technology was insufficient to achieve acceptable levels of

430 pollution decrease. Thus, the further development of integrated different techniques is  
431 in demand for taking into account a technically and economically feasible option. The  
432 experiment proved that this method was convenient and efficient for primary or deep  
433 treatment of wastewater. Coupling with a biological unit will be a promising way,  
434 which can obtain an effluent for its reuse or discharge to natural water sources.

435    **Acknowledgement**

436    This study was supported by National Natural Science Foundation of China

437    (51578223, 51378189 and 51521006).



438 **References**

- 439 1. R. Cossu, A. M. Polcaro, M. C. Lavagnolo, M. Mascia, S. Palmas and F.  
440 Renoldi, *Environ.sci.technol*, 1998, **32**, 3570-3573.
- 441 2. M. Panizza and C. A. Martinez-Huitle, *Chemosphere*, 2013, **90**, 1455-1460.
- 442 3. E. Turro, A. Giannis, R. Cossu, E. Gidarakos, D. Mantzavinos and A.  
443 Katsaounis, *Journal of hazardous materials*, 2012, **207**, 73-78.
- 444 4. J. Wu, H. Zhang, N. Oturan, Y. Wang, L. Chen and M. A. Oturan,  
445 *Chemosphere*, 2012, **87**, 614-620.
- 446 5. F. F. Cai, Z. H. Yang, H. Jing, G. M. Zeng, L. K. Wang and Y. Jian, *Journal of*  
447 *hazardous materials*, 2014, **275**, 63–71.
- 448 6. F. C. Moreira, J. Soler, A. Fonseca, I. Saraiva, R. A. R. Boaventura, E. Brillas  
449 and V. J. P. Vilar, *Water research*, 2015, **81**, 375-387.
- 450 7. A. Anglada, A. Urtiaga, I. Ortiz, D. Mantzavinos and E. Diamadopoulos,  
451 *Water research*, 2011, **45**, 828-838.
- 452 8. A. Coors, P. D. Jones, J. P. Giesy and H. T. Ratte, *Environmental Science &*  
453 *Technology*, 2003, **37**, 3430-3434.
- 454 9. J. L. de Morais and P. P. Zamora, *Journal of hazardous materials*, 2005, **123**,  
455 181-186.
- 456 10. H. Zhang, X. Ran, X. Wu and D. Zhang, *Journal of hazardous materials*,  
457 2011, **188**, 261-268.

- 458 11. A. Cabeza, A. Urtiaga, M. J. Rivero and I. Ortiz, *Journal of hazardous*  
459 *materials*, 2007, **144**, 715-719.
- 460 12. F. C. Moreira, J. Soler, A. Fonseca, I. Saraiva, R. A. R. Boaventura, E. Brillas  
461 and V. J. P. Vilar, *Applied Catalysis B: Environmental*, 2016, **182**, 161-171.
- 462 13. P. Marco and C. Giacomo, *Chemical Reviews*, 2009, **109**, 6570-6631.
- 463 14. N. Oturan, E. D. V. Hullebusch, H. Zhang, L. Mazeas, H. Budzinski, K. L.  
464 Menach and M. A. Oturan, *Environ.sci.technol*, 2015.
- 465 15. A. Fernandes, D. Santos, M. J. Pacheco, L. Ciriaco and A. Lopes, *Applied*  
466 *Catalysis B-Environmental*, 2014, **148**, 288-294.
- 467 16. E. Turro, A. Giannis, R. Cossu, E. Gidarakos, D. Mantzavinos and A.  
468 Katsaounis, *Journal of hazardous materials*, 2011, **190**, 460-465.
- 469 17. S. M. Moon and S. I. Pyun, *Corrosion Science*, 1997, **39**, 399-408.
- 470 18. M. Mokaddem, P. Volovitch, F. Rechou, R. Oltra and K. Ogle, *Electrochimica*  
471 *Acta*, 2010, **55**, 3779-3786.
- 472 19. W. G. Walter, *American Journal of Public Health & the Nations Health*, 1961,  
473 940.
- 474 20. J. Wu, H. Zhang, N. Oturan, Y. Wang, L. Chen and M. A. Oturan,  
475 *Chemosphere*, 2012, **87**, 614-620.
- 476 21. X. Mo, Z. H. Yang, H. Y. Xu, G. M. Zeng, J. Huang, X. Yang, P. P. Song and L.  
477 K. Wang, *Journal of hazardous materials*, 2015, **286**, 493-502.

- 478 22. T. F. C. V. Silva, A. Fonseca, I. Saraiva, R. A. R. Boaventura and V. J. P. Vilar,  
479 *Chemical Engineering Journal*, 2016, **283**, 76-88.
- 480 23. B. Cercado-Quezada, M.-L. Delia and A. Bergel, *Electrochemistry*  
481 *Communications*, 2011, **13**, 440-443.
- 482 24. H. Wang, S. Yuan, J. Zhan, Y. Wang, G. Yu, S. Deng, J. Huang and B. Wang,  
483 *Water research*, 2015, **80**, 20-29.
- 484 25. L. R. Czarnetzki and L. J. J. Janssen, *Journal of Applied Electrochemistry*,  
485 1992, **22**, 315-324.
- 486 26. G. Mouedhen, M. Feki, M. D. Petris-Wery and H. F. Ayedi, *Journal of*  
487 *hazardous materials*, 2009, **168**, 983–991.
- 488 27. Z. Zaroual, H. Chaair, A. H. Essadki, K. E. Ass and M. Azzi, *Chemical*  
489 *Engineering Journal*, 2009, **148**, 488-495.
- 490 28. L. C. Chiang, J. E. Chang and T. C. Wen, *Water research*, 1995, **29**, 671–678.
- 491 29. F. Feki, F. Aloui, M. Feki and S. Sayadi, *Chemosphere*, 2009, **75**, 256-260.
- 492 30. D. Yang and J. D. Englehardt, *Waste management*, 2007, **27**, 380–388.
- 493 31. P. B. Moraes and R. Bertazzoli, *Chemosphere*, 2005, **58**, 41-46.
- 494 32. G. Del Moro, L. Prieto-Rodríguez, M. De Sanctis, C. Di Iaconi, S. Malato and  
495 G. Mascolo, *Chemical Engineering Journal*, 2016, **288**, 87-98.
- 496 33. H. Zhang, Y. Li, X. Wu, Y. Zhang and D. Zhang, *Waste management*, 2010,  
497 **30**, 2096-2102.

- 498 34. J. E. Silveira, J. A. Zazo, G. Pliego, E. D. Bidóia and P. B. Moraes,  
499 *Environmental Science & Pollution Research International*, 2014, **22**,  
500 5831-5841.
- 501 35. E. Turro, A. Giannis, R. Cossu, E. Gidarakos, D. Mantzavinos and A.  
502 Katsaounis, *Journal of hazardous materials*, 2011, **190**, 460-465.
- 503 36. N. Fan, Z. Li, L. Zhao, N. Wu and T. Zhou, *Chemical Engineering Journal*,  
504 2013, **214**, 83-90.
- 505 37. M. Li, C. Feng, Z. Zhang and N. Sugiura, *Electrochimica Acta*, 2009, **54**,  
506 4600-4606.
- 507 38. A. A. Bukhari, *Bioresource technology*, 2008, **99**, 914-921.
- 508 39. H. Zhang, X. Ran, X. Wu and D. Zhang, *Journal of hazardous materials*,  
509 2011, **188**, 261-268.
- 510 40. Y. Lei, Z. Shen, R. Huang and W. Wang, *Water research*, 2007, **41**,  
511 2417-2426.
- 512 41. S. Aoudj, A. Khelifa, N. Drouiche, R. Belkada and D. Miroud, *Chemical*  
513 *Engineering Journal*, 2015, **267**, 153-162.
- 514 42. H. Zoellig, A. Remmele, C. Fritzsche, E. Morgenroth and K. M. Udert,  
515 *Environmental Science & Technology*, 2015, **49**, 11062-11069.
- 516 43. J. A. Gomes, P. Daida, M. Kesmez, M. Weir, H. Moreno, J. R. Parga, G. Irwin,  
517 H. McWhinney, T. Grady, E. Peterson and D. L. Cocke, *Journal of hazardous*  
518 *materials*, 2007, **139**, 220-231.

- 519 44. A. Fernandes, M. J. Pacheco, L. Ciriaco and A. Lopes, *Applied Catalysis B:*  
520 *Environmental*, 2015, **176-177**, 183-200.
- 521 45. A. Angela, U. Ane and O. Inmaculada, *Environ.sci.technol*, 2009, **43**,  
522 2035-2040.
- 523 46. Y. Gendel and O. Lahav, *Electrochimica Acta*, 2012, **63**, 209-219.
- 524 47. T. Picard, ., G. Cathalifaud-Feuillade, ., M. Mazet, . and C. Vandensteendam, .  
525 *Journal of Environmental Monitoring Jem*, 2000, **2**, 77-80.
- 526 48. S. O. Klemm, J. P. Kollender and A. Walter Hassel, *Corrosion Science*, 2011,  
527 **53**, 1-6.
- 528

### Figure captions

**Fig. 1** Schematic of a simplified reactor that represented the design of electrochemical reactor.

**Fig. 2** Effects of electrode materials, electrolytic time on COD,  $\text{NH}_3\text{-N}$  (a) and color (b) removal, and effect of electrode gap on COD and  $\text{NH}_3\text{-N}$  removal (c).

**Fig. 3** 3D surface plots for COD (a~c) and  $\text{NH}_3\text{-N}$  (d~f) removal efficiency as a function of two independent variables (other variables were held at their respective center levels).

**Fig. 4** GC-MS analysis of leachate before and after electrochemical experiment.

**Fig. 5** (a) ESEM image, (b) EDS spectra and (c) FT-IR spectra of the sludge generated in the electrochemical process.

**Fig. 6** The reaction mechanism responsible for the removal of pollutants.

**Fig. 7** pH and chloride ion concentration variations in the process of electrolysis.

**Fig. 8** Electrical energy consumption for the treatment of landfill leachate.

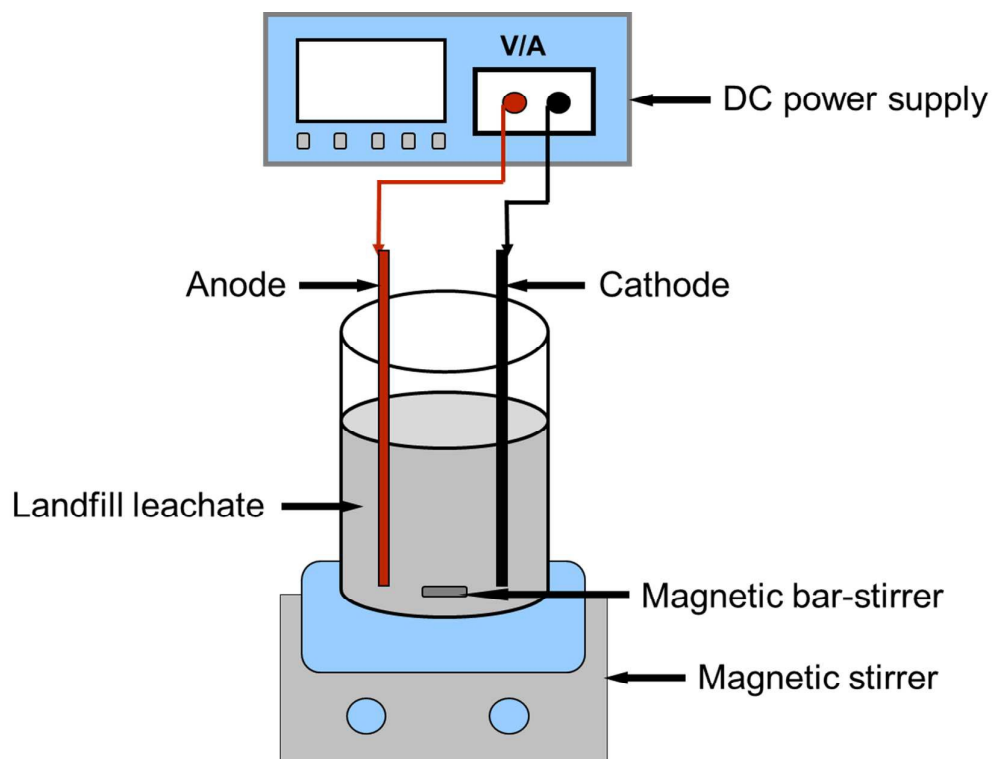
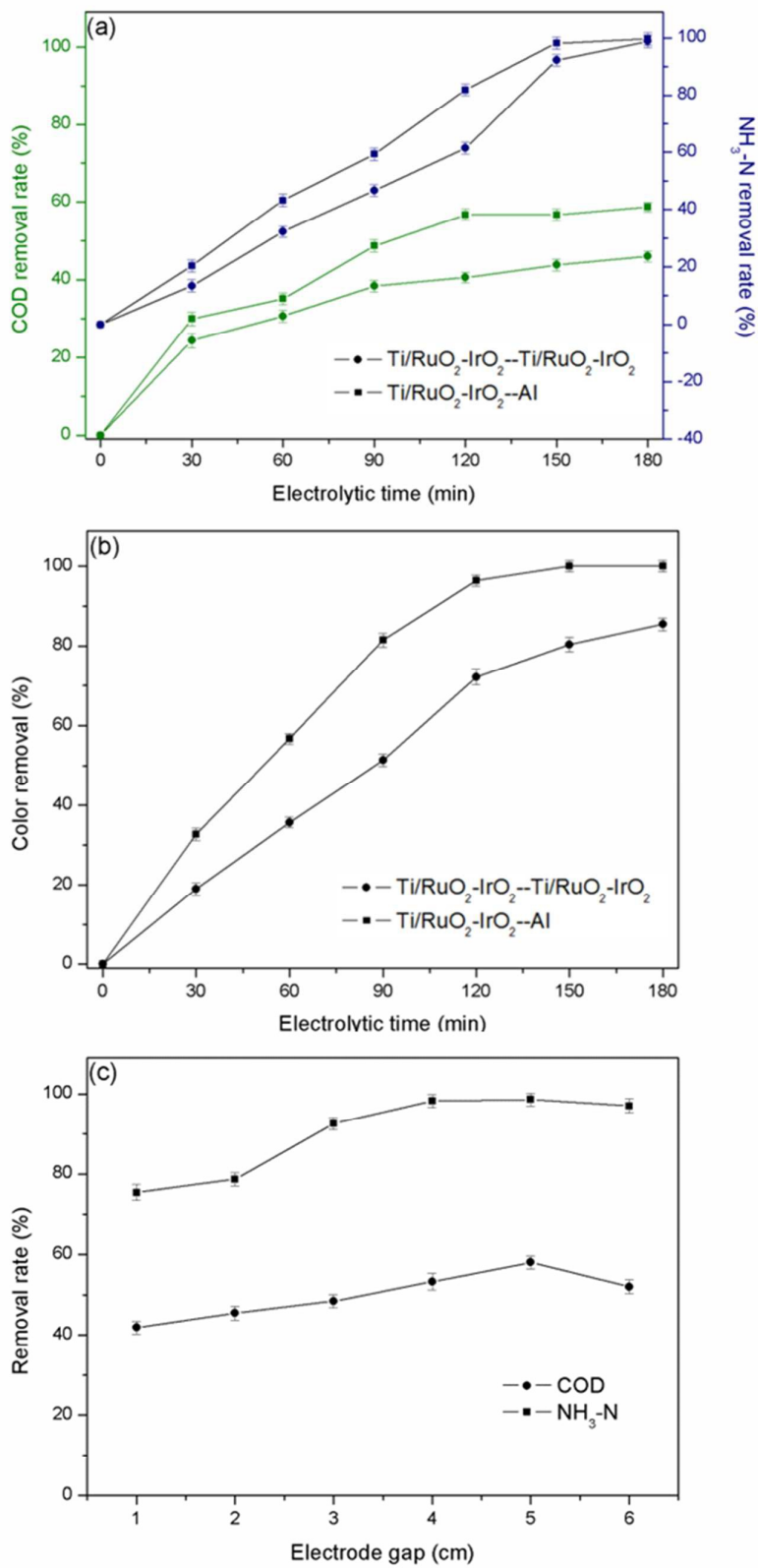


Fig. 1 Schematic of a simplified reactor that represented the design of electrochemical reactor.



**Fig. 2** Effects of electrode materials, electrolytic time on COD, NH<sub>3</sub>-N (a) and color (b) removal, and effect of electrode gap on COD and NH<sub>3</sub>-N removal (c).



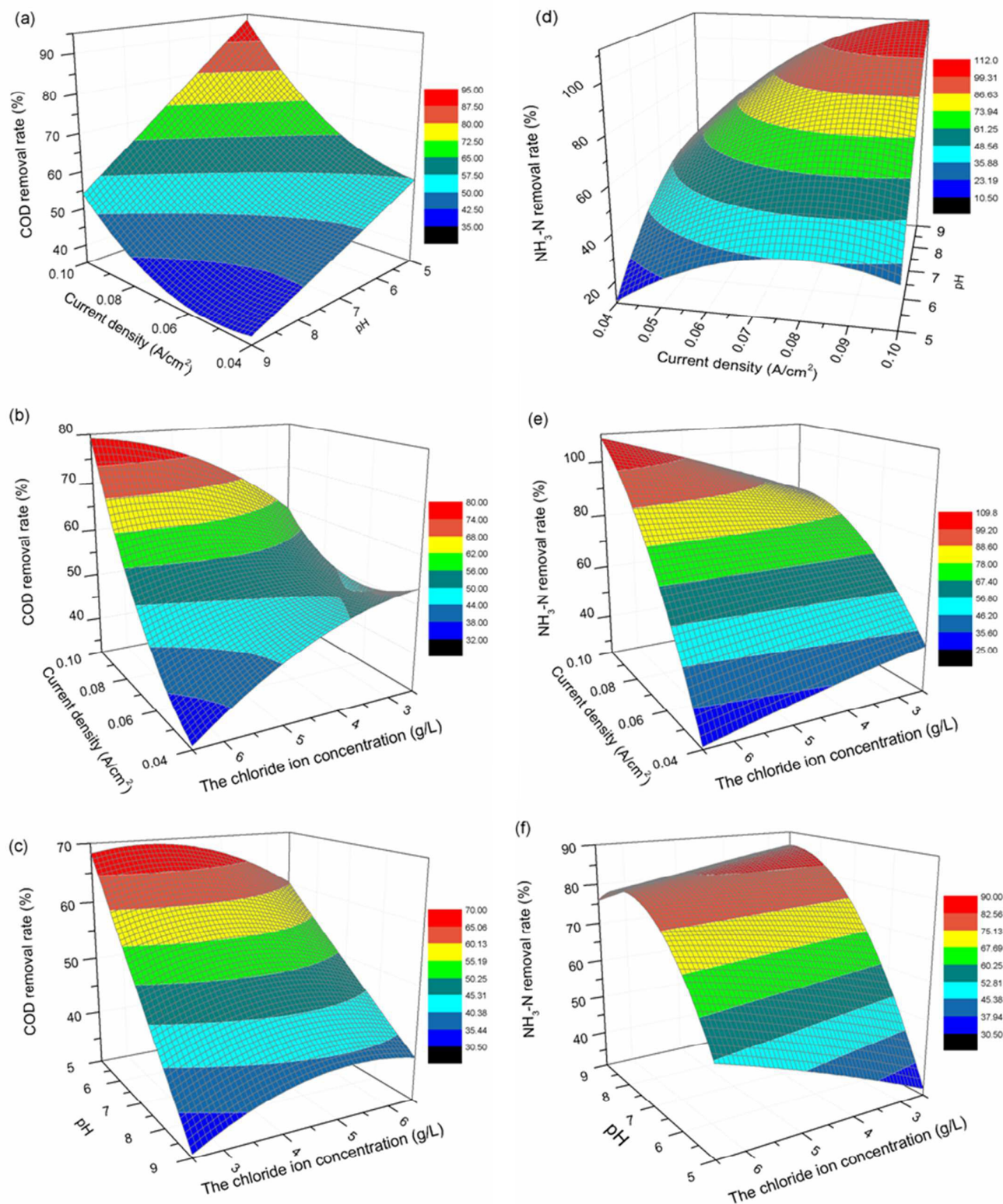


Fig. 3 3D surface plots for COD (a~c) and  $\text{NH}_3\text{-N}$  (d~f) removal efficiency as a function of two independent variables (other variables were held at their respective center levels).

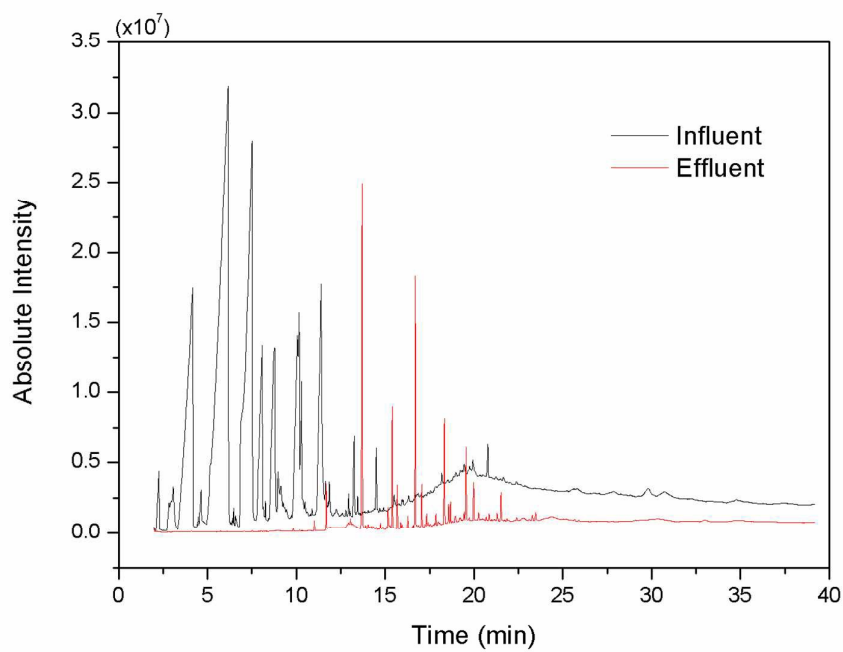


Fig. 4 GC-MS analysis of leachate before and after electrochemical experiment.

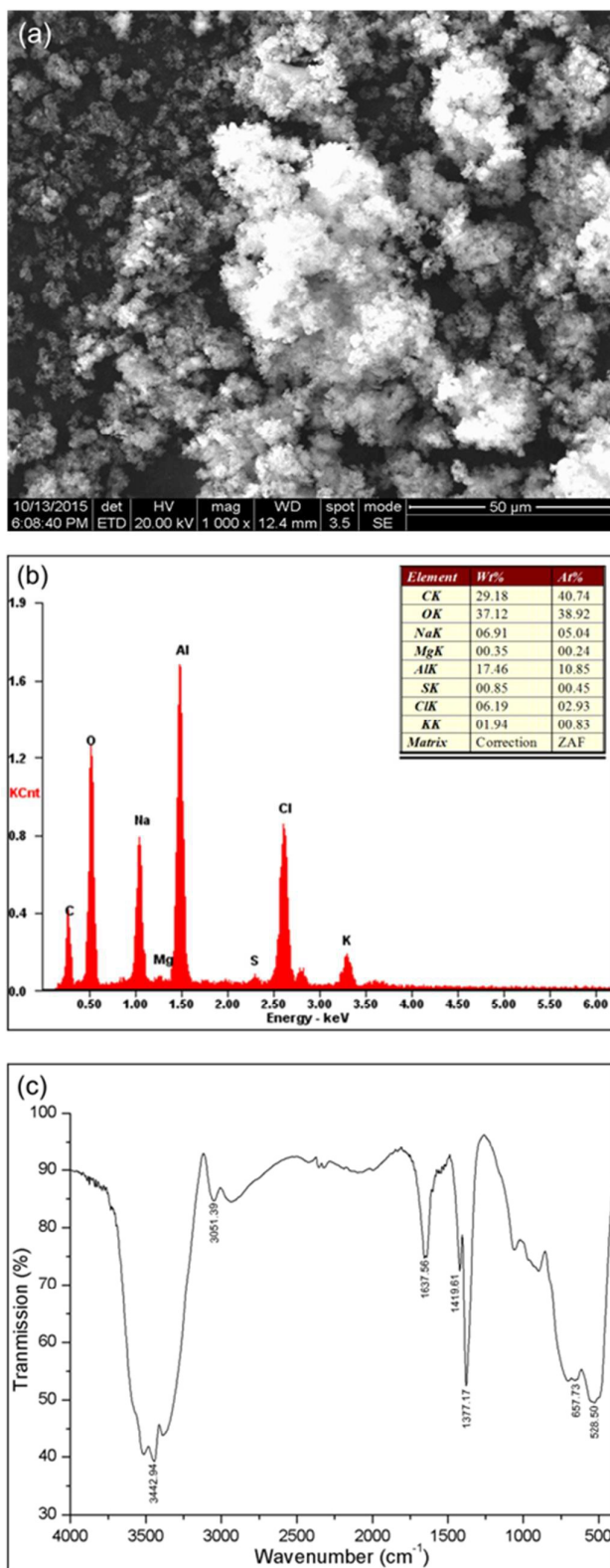


Fig. 5 (a) ESEM image, (b) EDS spectra and (c) FT-IR spectra of the sludge generated in the electrochemical process.

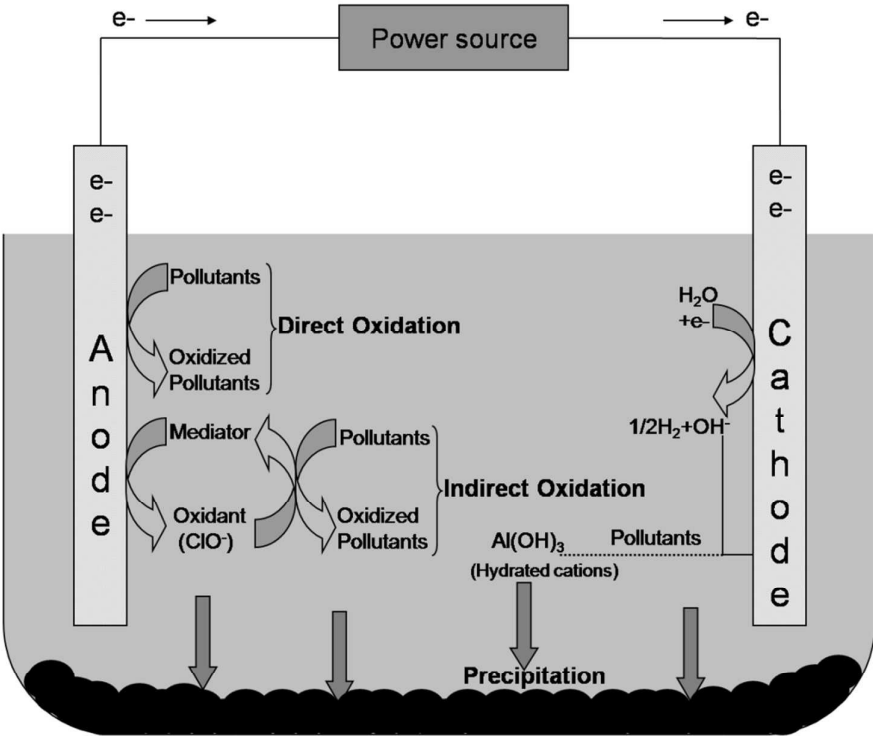


Fig. 6 The reaction mechanism responsible for the removal of pollutants.

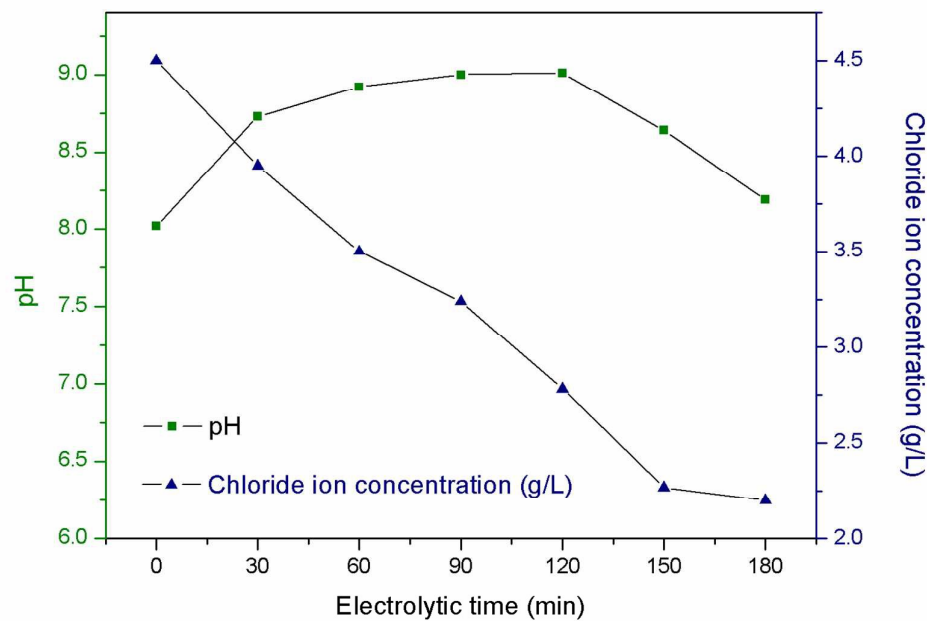


Fig. 7 pH and chloride ion concentration variations in the process of electrolysis.

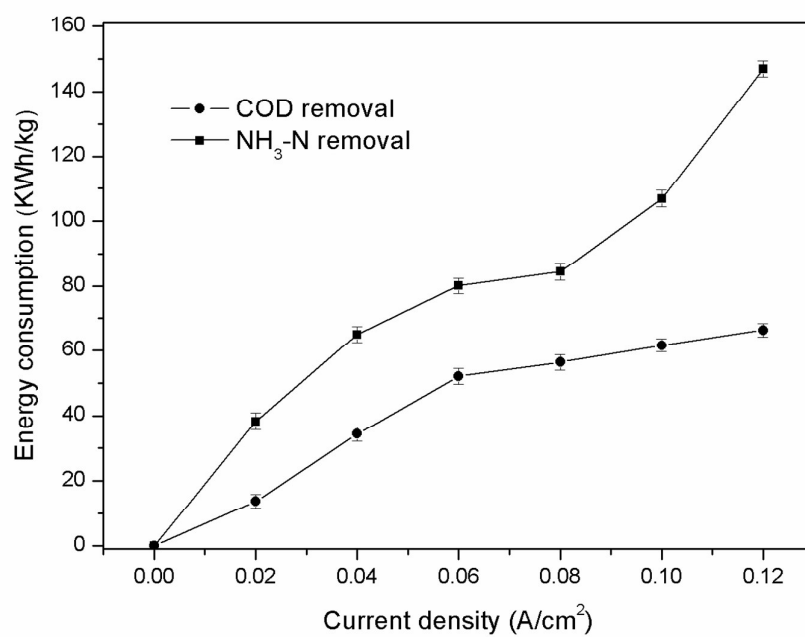


Fig. 8 Electrical energy consumption for the treatment of landfill leachate.

**Table 1** The characteristics of leachate samples.

Parameters	Unit	Range	Average
pH	-	7.80~8.28	8.04
Conductivity	mS/cm	12.05~13.08	12.62
Cl <sup>-</sup>	mg/L	2300~2800	2500
BOD <sub>5</sub>	mg/L	440~520	480
COD	mg/L	3640~4296	3968
BOD <sub>5</sub> /COD	-	0.10~0.14	0.12
NH <sub>3</sub> -N	mg/L	1840~2042	2000
Sodium	g/L	3.528~3.800	3.664
Potassium	g/L	1.264~1.386	1.325

**Table 2** Experimental range and levels of the independent variables.

Variables		Range and level				
		-1.682	-1	0	1	1.682
Current density(A/cm <sup>2</sup> )	$x_1$	0.04	0.05	0.07	0.09	0.1
pH	$x_2$	5.00	5.81	7.00	8.19	9.00
The chloride ion concentration(g/L)	$x_3$	2.50	3.31	4.50	5.60	6.50

**Table 3** ANOVA results for response surface quadratic model analysis of variance.

	Source	Sum of Squares	Degree of freedom	Mean Square	F-Value	Prob>F	
COD removal (%)	Model	2186.53	9	242.95	22.78	< 0.0001	significant
	$x_1$	845.93	1	845.93	79.32	< 0.0001	
	$x_2$	1074.18	1	1074.18	100.72	< 0.0001	
	$x_3$	0.49	1	0.49	0.046	0.8343	
	$x_1x_2$	22.51	1	22.51	2.11	0.1769	
	$x_1x_3$	99.55	1	99.55	9.33	0.0121	
	$x_2x_3$	13.42	1	13.42	1.26	0.2883	
	Residual	106.65	10	10.67			
	Lack of Fit	87.06	5	17.41	4.44	0.0637	not significant
	Pure Error	19.60	5	3.92			
S.D.=3.27, PRESS=690.55, $R^2=0.9535$ , $R^2_{adj}=0.9116$ , Adeq precision=16.430.							
NH <sub>3</sub> -N removal (%)	Model	7246.63	9	805.18	43.19	< 0.0001	significant
	$x_1$	4586.53	1	4586.53	246.04	< 0.0001	
	$x_2$	1818.37	1	1818.37	97.55	< 0.0001	
	$x_3$	28.50	1	28.50	1.53	0.2445	
	$x_1x_2$	104.84	1	104.84	5.62	0.0392	
	$x_1x_3$	107.75	1	107.75	5.78	0.0370	
	$x_2x_3$	58.54	1	58.54	3.14	0.1068	
	Residual	186.41	10	18.64			
	Lack of Fit	180.50	5	36.10	30.55	0.0009	significant
	Pure Error	5.91	5	1.18			
S.D.=4.32, PRESS=1533.46, $R^2=0.9749$ , $R^2_{adj}=0.9524$ , Adeq precision=22.476.							

**Table 4** Optimum conditions found by design expert and verification for COD and NH<sub>3</sub>-N removals.

Response	Current density (A/cm <sup>2</sup> )	pH	The chloride ion concentration (g/L)	Removal rate (%)		Error	Desirability
				Predicted	Observed		
COD	0.10	6.37	6.50	84.26	83.93	0.33	87.2%
NH <sub>3</sub> -N	0.10	6.37	6.50	100	100	0.00	87.2%



Table 5 The research results previously reported for the degradation of leachates by electrochemical oxidation under the different cathode.

Anode	Cathode	Current density (A/cm <sup>2</sup> )	pH	Reaction time (min)	Initial COD concentration (mg/L)	COD removal (%)	Initial NH <sub>3</sub> -N concentration (mg/L)	NH <sub>3</sub> -N removal (%)	References
Ti/RuO <sub>2</sub> – IrO <sub>2</sub>	Ti	0.116	8.25	180	1855	73	1060	49	[31]
Ti/RuO <sub>2</sub> – IrO <sub>2</sub>	Ti/RuO <sub>2</sub> – IrO <sub>2</sub>	0.200	8.60	240	3973	87.4	1726.6	NS	[32]
Ti/RuO <sub>2</sub> – IrO <sub>2</sub>	stainless steel	0.060	8.40	180	2091	20.2	2531	57.7	[33]
Ti/RuO <sub>2</sub> – IrO <sub>2</sub>	stainless steel	0.244	7.60	41.78	1375	54.99	1200	71.07	[34]
Ti/ RuO <sub>2</sub> – IrO <sub>2</sub>	Zr	0.032	3.00	240	2960	65	14	NS	[35]
Ti/ RuO <sub>2</sub> – IrO <sub>2</sub>	Cu/Zn	0.025	7.80	360	NA	NA	60	95.98	[36,37]
Ti/ RuO <sub>2</sub> – IrO <sub>2</sub>	Fe	0.020	7.00	180	NA	NA	100	87	[37]

NA-Not applied; NS-not specified

**Table 6** Heavy metals removal from landfill leachate using Ti/RuO<sub>2</sub>-IrO<sub>2</sub> and Al electrode in optimum conditions.

Species	Initial concentration (mg/L)	Final concentration (mg/L)	Removal rate (%)
Fe	14.90	0.06	99.60
B	2.80	2.00	28.27
Al	0.70	0.00	100.00
Ni	0.30	0.02	93.33
Zn	0.30	0.25	16.67
Cr	0.30	0.20	33.33
As	0.20	0.01	95.00
Pb	0.10	0.01	90.00
Co	0.08	0.00	100.00
Se	0.05	0.01	80.00
Cu	0.02	0.00	100.00